

Quantum critical points of Helical Fermi Liquids

Cenke Xu¹

¹*Department of Physics, Harvard University, Cambridge, MA 02138*

(Dated: November 24, 2018)

Following our previous work, we study the quantum phase transitions which spontaneously develop ferromagnetic spin order in helical fermi liquids which breaks continuous spin-space rotation symmetry, with application to the edge states of 3d topological band insulators. With finite fermi surface, the critical point has both $z = 3$ over-damped and $z = 2$ propagating quantum critical modes, and the $z = 3$ mode will lead to non-fermi liquid behavior on the entire fermi surface. In the ordered phase, the Goldstone mode is over-damped unless it propagates along special directions, and quasiparticle is ill defined on most parts of the fermi surface except for special points. Generalizations of our results to other systems with spin-orbit couplings are also discussed.

PACS numbers:

Helical fermi liquids (FL) have momentum dependent spin or pseudospin alignments at the fermi surface. For instance, the well-studied Rashba model [1, 2]

$$H = \frac{k^2}{2m} + \alpha(k_x\sigma^y - k_y\sigma^x) \quad (1)$$

have inner and outer fermi surfaces with opposite inplane helical spin direction. Another example of helical FL is the edge states of 3d topological band insulators (TBI) like $\text{Bi}_{2-x}\text{Sn}_x\text{Te}_3$ [3, 4, 5, 6], which can be described by the following Dirac fermion Hamiltonian

$$H = v_f(k_x\sigma^y - k_y\sigma^x) \quad (2)$$

v_f is the fermi velocity at the Dirac point. When the chemical potential is nonzero, the spin σ^a of the electrons are perpendicular with their momenta at the fermi surface (Fig. 1). Eq. 2 is the minimal model of helical FL because it has only one fermi surface, and the time-reversal partner of this model is located on the opposite edge of the three dimensional TBI. Recent ARPES measurement [7] has successfully observed the helical spin alignment of the edge states of 3d TBI. Both the Rashba model and Eq. 2 are invariant under the following symmetry transformations:

$$T : t \rightarrow -t, k_i \rightarrow -k_i, \sigma^a \rightarrow -\sigma^a,$$

$$P_x : x \rightarrow -x, \sigma^x \rightarrow \sigma^x, \sigma^y \rightarrow -\sigma^y,$$

$$P_y : y \rightarrow -y, \sigma^y \rightarrow \sigma^y, \sigma^x \rightarrow -\sigma^x,$$

$$R_\theta : (x, y)^t \rightarrow e^{i\theta\tau^2}(x, y)^t, \sigma^a \rightarrow e^{-i\frac{\theta}{2}\sigma^z}\sigma^a e^{i\frac{\theta}{2}\sigma^z}. \quad (3)$$

T, P_a are discrete symmetry transformation, while R_θ continuously rotate spin and space by the same angle θ , which corresponds to the conservation of total angular momentum. In this work we will take the edge states of the TBI as an example of helical FL, but our results can be straightforwardly generalized to other situations.

Just like the ordinary fermi liquid, strong enough interaction can lead to various types of instabilities of helical

FL, which spontaneously break all or part of the symmetries listed in Eq. 3. Supposedly strong interaction will play an important role in the TBI with transition metal elements, where the interplay between spin-orbit coupling and interaction can lead to many interesting phenomena [8, 9]. According to the standard Hertz-Millis theory [10, 11], for ordinary fermi liquid, the quantum critical modes are usually over-damped due to low energy particle-hole excitations, which lead to nonrelativistic universality class. In a recent paper we studied the discrete time reversal symmetry breaking of the helical FL [12], and the helical spin alignment at the fermi surface strongly suppresses the coupling between order parameter and the particle-hole excitations. Therefore the T-breaking phase transition belongs to the $z = 1$ 3d Ising universality class. In the current paper we will study the phase transition that breaks the continuous symmetry R_θ in Eq. 3, which is associated with the inplane ferromagnetic spin order $\vec{\phi} = (\phi_x, \phi_y)$. Identifying the leading spin order instability of the helical FL requires the detailed knowledge of the fermion interaction. As in our previous work, we will focus on the universal physics at the quantum critical point, assuming the existence of the phase transition.

Without loss of generality, the Lagrangian describing this transition can be written as

$$L = L_f + L_b + L_{bf},$$

$$L_f = \psi^\dagger((i\partial_t - \mu) + iv_f\hat{z} \cdot (\vec{\sigma} \times \vec{\nabla}))\psi,$$

$$L_b = |\partial_t\vec{\phi}|^2 - \sum_{i=x,y} v_b^2|\partial_i\vec{\phi}|^2 - r|\vec{\phi}|^2 - u|\vec{\phi}|^4,$$

$$L_{bf} = g\vec{\phi} \cdot \psi^\dagger\vec{\sigma}\psi. \quad (4)$$

The order parameter $\vec{\phi}$ couples with the Dirac current, which is similar to the 3d QED with gauge field $a_\mu = (\phi_y, -\phi_x, 0)$ and the temporal gauge choice $a_0 = 0$. The temporal component a_0 represents the charge density mode, which will couple to the XY spin mode after integrating out fermions. The implication of the spin-charge

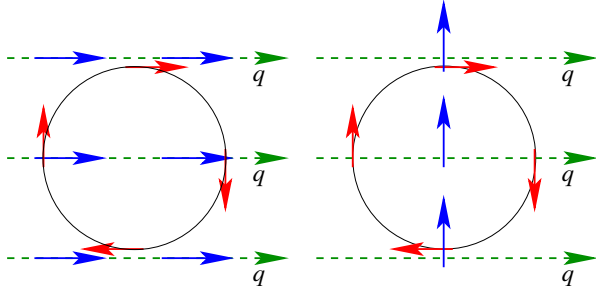


FIG. 1: The Fermi surface of helical FL, with finite chemical potential. The green dashed arrow is the direction of momentum \vec{q} carried by $\vec{\phi}_{\vec{q}}$, the blue arrow is the direction of $\vec{\phi}$, the red arrow represents the helical spin direction on the Fermi surface. (Left), a longitudinal mode of $\vec{\phi}$ with $\vec{\phi}$ parallel to \vec{q} interacts strongly with the helical Fermi liquid close to $\vec{K}_f \perp \vec{q}$, where the spin is parallel to $\vec{\phi}$; (Right), a transverse mode of $\vec{\phi}$ interacts weakly with helical Fermi liquid.

coupling has been studied in Ref. [13, 14]. However, at the frequency and momentum range we are interested in, the charge mode will not lead to singular corrections to the spin response function, *i.e.* the charge mode is not critical. The transition occurs when $r = 0$. Let us take $\mu = 0$ first. L_b alone describes a 3d XY transition, but g is obviously relevant at the 3d XY and free Dirac fermion fixed point based on the well-known scaling dimensions $[\psi] = 1$ and $[\phi] = 0.519$ [15], this fermion-boson coupling will modify the nature of this transition. A controlled starting point for the calculation of critical exponents, is to increase the number of fermion components to $N > 1$, and take the large- N limit. After integrating out the fermions, the renormalized boson Lagrangian reads

$$L_b \sim N \tilde{P}_{ab} \sqrt{\omega^2 + v_f^2 q^2} \phi_{a,\omega,\vec{q}} \phi_{b,-\omega,-\vec{q}} + \dots$$

$$\tilde{P}_{ab} = \frac{\omega^2 \delta_{ab} + v_f^2 q_a q_b}{\omega^2 + v_f^2 q^2}, \quad (5)$$

In the large- N limit the scaling dimension of $\vec{\phi}$ is $[\phi] = 1$. A standard $1/N$ expansion calculation can be applied to the case with large but finite N , although when $N = 1$ there is no small parameter for expansion. Phase transitions with order parameters coupled to certain component of Dirac current were studied in the context of d -wave superconductor by $1/N$ expansion [16, 17], and a fixed point with extreme anisotropic Fermi velocity was found if we start with an anisotropic initial condition [18].

Now let us consider the situation with $\mu \neq 0$, *i.e.* the situation with finite Fermi surface. In the ordinary Fermi liquid, an order parameter with small momentum $|\vec{q}| \ll k_f$ interacts most strongly with fermions at $\vec{K}_f \perp \vec{q}$, because there the particle-hole excitation at momentum \vec{q} is softest, and usually leads to over-damping of the quantum critical modes. In our current case, since the spin alignment at the Fermi surface is determined by its mo-

mentum, not all quantum critical modes have strong interactions with the fermions. For instance, for a quantum critical mode with $\vec{\phi}$ and momentum \vec{q} both parallel to \hat{x} , it couples with the fermions at two points $\vec{K}_f = (0, \pm k_f)$ in the same way as the ordinary Fermi liquid, therefore the longitudinal mode of $\vec{\phi}$ is over-damped (Fig. 1). If $\vec{\phi}$ is parallel with \hat{y} while \vec{q} parallel with \hat{x} , since the matrix element $\langle \psi_{\vec{k}} | \sigma^y | \psi_{\vec{k}} \rangle = 0$ when $\vec{k} = (0, \pm k_f)$, the transverse mode of $\vec{\phi}$ should couple weakly with the fermions. These observations suggest that after integrating out the fermions, the transverse and longitudinal modes of $\vec{\phi}$ will behave differently. Indeed, the $L_f + L_{bf}$ part of the Lagrangian Eq. 4 is invariant under gauge transformation

$$\phi_a \rightarrow \phi_a + \epsilon_{ab} \partial_b \theta, \quad \psi \rightarrow e^{i\theta} \psi, \quad (6)$$

and θ is an arbitrary function of space. If we integrate out the fermions, and consider a Feynman diagram without boson internal line, this gauge symmetry implies that any external boson line of this diagram only involves the longitudinal mode of $\vec{\phi}$ when the frequency of this external line is zero. For instance, Eq. 5 is consistent with this conclusion, because $\tilde{P}_{ab} \epsilon_{bc} q_c = 0$ when $\omega = 0$.

The above observation becomes explicit in the bubble diagram in Fig. 2a, which renormalizes the Gaussian part of L_b as

$$\Delta L_b \sim \phi_{a,-\omega,-\vec{q}} \chi(\omega, \vec{q})_{ab} \phi_{b,\omega,\vec{q}}. \quad (7)$$

If we fix chemical potential μ and the energy at the ultraviolet cut-off, the calculation suggests that the static and uniform susceptibility $\chi(0, 0)$ vanishes, which can be naturally expected because a uniform order of $\vec{\phi}$ merely moves the entire Dirac cone away from the original position, without developing any extra polarization on the Fermi surface. This calculation implies that the mass gaps of transverse and longitudinal modes are still equal after coupling to the fermions, because a different mass gap for these two modes will lead to very singular long range interaction between $\vec{\phi}$ in real space-time. In the ordinary Hertz-Millis theory [10, 11] of quantum phase transition inside Fermi liquid, the most singular correction to the effective Lagrangian of order parameter comes from the imaginary part of the susceptibility, which corresponds to the damping of the critical mode of order parameter $\vec{\phi}$ through particle-hole excitations. The damping rate can be calculated from the Feynman diagram Fig. 2b, or through the Fermi-Golden rule

$$\begin{aligned} \text{Im}[\Sigma_{\vec{\phi}}(\omega, q)_{ab}] &\sim \int \frac{d^2 k}{(2\pi)^2} [f(\epsilon_{k+q}) - f(\epsilon_k)] \\ &\times g^2 \delta(|\omega| - \epsilon_{k+q} + \epsilon_k) \mathcal{M}_{k,k+q}^a \mathcal{M}_{k+q,k}^b \\ &\sim g^2 \frac{|\omega|}{v_f q} P_{ab} + g^2 \frac{|\omega|^3}{v_f^3 q^3} (\delta_{ab} - P_{ab}), \\ M_{k,k+q}^a &= \langle k | \psi_k^\dagger \sigma^a \psi_{k+q} | k+q \rangle, \end{aligned}$$

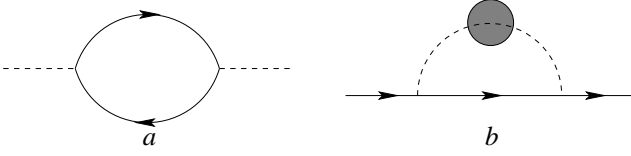


FIG. 2: *a*, the bubble diagram for the self-energy correction to $\vec{\phi}$; *b*, the self-energy correction to fermions.

$$P_{ab} = \frac{q_a q_b}{q^2}. \quad (8)$$

Matrix P_{ab} projects $\vec{\phi}$ to its longitudinal part, and P satisfies the algebraic relation $P^2 = P$. This calculation indicates that only the longitudinal part of $\vec{\phi}$ is over-damped, while the transverse part of $\vec{\phi}$ gains a much weaker damping as $\omega/(v_f q) \rightarrow 0$, which is consistent with our observation. The decomposition between transverse and longitudinal modes also occurs in a very different problem: the nematic transition of fermi liquid [19].

The real part of self-energy can be calculated accordingly. The result in the infrared limit depends on how we take the limit of the frequency and momentum. In the limit $\omega/(v_f q) \ll 1$, the result reads

$$\begin{aligned} \text{Re}[\Sigma_{\vec{\phi}}(\omega, q)_{ab}] &\sim \int \frac{d^2 k}{(2\pi)^2} \frac{[f(\epsilon_{k+q}) - f(\epsilon_k)](\epsilon_{k+q} - \epsilon_k)}{\omega^2 - (\epsilon_{k+q} - \epsilon_k)^2} \\ &\times g^2 \mathcal{M}_{k,k+q}^a \mathcal{M}_{k+q,k}^b \\ &\sim g^2 \int d\theta \frac{F(\theta)_{ab}}{\frac{\omega^2}{v_f^2 q^2} - [\cos(\theta)]^2} \\ &\sim -g^2 \frac{\omega^2}{q^2} P_{ab} + g^2 \frac{\omega^2}{q^2} (\delta_{ab} - P_{ab}) + \dots \end{aligned} \quad (9)$$

$F(\theta)_{ab}$ is a spin dependent function of θ (the angle between \vec{k} and \vec{q}). The ellipses include less singular terms. The transverse mode and longitudinal mode both acquire singular correction ω^2/q^2 . The ω^2/q^2 behavior is the reason of the existence of various collective modes of the ordinary fermi liquid, such as the zero sound. In our previous paper about the Ising transition [12], the ω^2/q^2 term does not show up because the matrix element $|\langle k|\sigma^z|k+q\rangle|^2 \sim q^2$ with small q , which cancels the q^2 in the denominator. Keeping all the relevant terms from imaginary and real parts, the full Gaussian Lagrangian for $\vec{\phi}$ in the Euclidean space-time reads

$$\begin{aligned} L_b &\sim (Ag^2 \frac{|\omega|}{v_f q} + v_l^2 q^2) P_{ab} \phi_{a,-\omega,-\vec{q}} \phi_{b,\omega,\vec{q}} \\ &+ (Bg^2 \frac{\omega^2}{v_f^2 q^2} + v_t^2 q^2) (\delta_{ab} - P_{ab}) \phi_{a,-\omega,-\vec{q}} \phi_{b,\omega,\vec{q}} \end{aligned} \quad (10)$$

A and B are order one dimensionless constants, v_l and v_t are renormalized boson velocities. The renormalized

propagator of $\vec{\phi}$ reads

$$D(\omega, \vec{q})_{ab} \sim \frac{P_{ab}}{Ag^2 \frac{|\omega|}{v_f q} + v_l^2 q^2} + \frac{\delta_{ab} - P_{ab}}{Bg^2 \frac{\omega^2}{v_f^2 q^2} + v_t^2 q^2}. \quad (11)$$

This calculation suggests that by coupling to the helical FL, at the quantum critical point the longitudinal part of $\vec{\phi}$ becomes a $z = 3$ over-damped mode, while the transverse part of $\vec{\phi}$ becomes a $z = 2$ propagating mode. For both $z = 3$ and $z = 2$ scaling, $\omega/q \rightarrow 0$ with small frequency and momentum, which justifies the small $\omega/(v_f q)$ limit we took at the beginning of our calculation. Because $\chi(0, 0)$ vanishes, both transverse and longitudinal modes become gapless at the same critical point.

In two dimension, $z = 2$ quantum critical point is at the critical dimension, therefore the Gaussian fixed point Eq. 10 is stable with marginally irrelevant perturbations. As discussed in ordinary $z = 3$ and $z = 2$ quantum critical points, more singular perturbations may be generated with higher order fermion loop diagrams [20, 21]. These singular perturbations may also exist in our situation, we will discuss this possibility in future, right now we tentatively focus on one-loop result and ignore these terms. The $z = 3$ and $z = 2$ quantum critical modes define the quantum critical regime $T > |r|^{z\nu} \sim |r|^{3/2}$ and $T > |r|$ respectively, therefore in the quantum critical regime at low temperature the thermal dynamics is dominated by the $z = 3$ longitudinal mode, which leads to the specific heat scaling $C_v \sim T^{2/3}$.

In the quantum critical regime, the fermions interact strongly with the bosons, and gain self-energy renormalization. The self-energy renormalization can be calculated in the standard way using diagram Fig. 2b. Let us take the quasiparticle at $\vec{K}_f = (+k_f, 0)$, where the dispersion of quasiparticle can be expanded as $\epsilon_k \sim v_f k_x + v_y k_y^2$, therefore around this point k_x has scaling dimension 2 while k_y has scaling dimension 1. Since the spin is along the \hat{y} direction, in the calculation we should project the boson propagator in the \hat{y} direction. Using the propagator in Eq. 11, the fermion self-energy reads

$$\begin{aligned} \Sigma_\psi &\sim \int \frac{d^2 k d\nu}{(2\pi)^3} \frac{1}{i(\omega + \nu) - v_f(k_x + q_x) - v_y^2(k_y + q_y)^2} \\ &\times \left(\frac{P_{yy}}{Ag^2 \frac{|\omega|}{v_f k} + v_l^2 k^2} + \frac{1 - P_{yy}}{Bg^2 \frac{\omega^2}{v_f^2 k^2} + v_t^2 k^2} \right). \end{aligned} \quad (12)$$

The self-energy is dominated by the $z = 3$ longitudinal mode, which leads to the same self-energy scaling as the ordinary $z = 3$ quantum critical point:

$$\Sigma_\psi(\omega)'' \sim |\omega|^{2/3} \text{sgn}[\omega]. \quad (13)$$

The transverse mode will lead to a less singular correction $\Sigma_\psi(\omega) \sim \omega \log(|\omega|)$, which is the same as the marginal fermi liquid [22]. Therefore at the quantum critical point the system has non-fermi liquid behavior.

It is useful to discuss more about the isolated fermi patch around $\vec{K}_f = (+k_f, 0)$. As in Eq. 12, after projecting the boson propagator along \hat{y} direction, the transverse part of the propagator acquires a factor $1 - P_{yy} = k_x^2/(k_x^2 + k_y^2)$. Because now k_x has scaling dimension 2, the transverse part of the propagator is effectively suppressed. Therefore in the Lagrangian we can keep just the scalar longitudinal mode. Now the isolated patch is described by the following scaling invariant Lagrangian

$$\begin{aligned} L &= L_f + L_b + L_{bf}, \\ L_f &= \sum_{\omega, \vec{k}} (c|\omega|^{2/3} \text{sgn}[\omega] - v_f k_x - v_y k_y^2) \psi_{\omega, \vec{k}}^\dagger \psi_{\omega, \vec{k}}, \\ L_b &= \sum_{\omega, \vec{k}} (Ag^2 \frac{|\omega|}{v_f |k_y|} + v_l^2 k_y^2) \phi_{\omega, \vec{k}} \phi_{-\omega, -\vec{k}}, \\ L_{bf} &= \sum_{\omega, \nu, \vec{p}, \vec{q}} g \phi_{\omega, \vec{q}} \psi_{\nu+\omega, \vec{p}+\vec{q}}^\dagger \psi_{\vec{q}}. \end{aligned} \quad (14)$$

One can verify that under the scaling transformation $\omega \rightarrow \omega b^3$, $k_x \rightarrow k_x b^2$, $k_y \rightarrow k_y b$, $\psi \rightarrow \psi b^4$, $\phi \rightarrow \phi b^4$, $g \rightarrow g$ this Lagrangian is invariant. Therefore the coupling g is a marginal perturbation, and the theory becomes identical to the spinon and gauge field problem discussed in Ref. [23, 24]. In the large- N limit with N copies of the fermi patches, this theory is expected to be controlled by a strongly coupled CFT [23].

Now let us discuss the ordered phase, with $r < 0$ in Eq. 4. The low energy physics of the ordered phase is dominated by the Goldstone mode. Let us assume the order is $\langle \vec{\phi} \rangle \sim (0, \phi_y)$, and the Goldstone mode is ϕ_x . As already mentioned before, in the ordered phase, the entire Dirac cone is translated in the momentum space without change of the shape of fermi surface, therefore the Goldstone mode of ordered phase of $\vec{\phi}$ has a very similar behavior as the quantum critical mode:

$$L_{\phi_x} \sim Ag^2 \frac{i\omega q_x^2}{v_f q^3} + Bg^2 \frac{\omega^2}{v_f^2 q^2} \left(\frac{q_y^2 - q_x^2}{q^2} + D \frac{q_x^2 q_y^2}{|r| q^4} \right) - q^2 + \dots \quad (15)$$

When the momentum is along \hat{x} (longitudinal), this Goldstone mode is an over-damped $z = 3$ mode; when momentum is along \hat{y} (transverse), the Goldstone mode is a propagating $z = 2$ mode. In the ordered phase, the over-damped longitudinal Goldstone mode will lead to the same nonfermi liquid self-energy correction as Eq. 13 for almost all points on the fermi surface:

$$\Sigma_\psi(\omega)'' \sim |\cos(\phi)|^{4/3} |\omega|^{2/3} \text{sgn}[\omega], \quad (16)$$

ϕ is the angle between \vec{K}_f and $\vec{\phi}$. At the special points $\phi = \pm\pi/2$, the correction to the fermion self-energy mainly comes from the transverse part of the Goldstone mode, which reads

$$\Sigma_\psi(\omega)'' \sim |\omega|^{3/2} \text{sgn}[\omega]. \quad (17)$$

Therefore in the ordered phase only two special points of the fermi surface have well-defined quasiparticles. The results obtained here in the ordered XY phase are similar to the nematic transition in 2d fermi liquid [19].

So far we only kept the lowest order momentum dependent terms in Eq. 2, while in real system the symmetry R_θ is broken by lattice symmetry, as was shown by first principle calculations [25]. In $\text{Bi}_{2-x}\text{Sn}_x\text{Te}_3$ the continuous $O(2)$ symmetry of R_θ is broken down to C_6 inplane rotation symmetry with large chemical potential [4], and the spin will be canted along z direction except for isolated points on the fermi surface [25, 26]. In our previous work we have argued that the z direction canting will lead to damping of the Ising order parameter $\phi \sim \psi^\dagger \sigma^z \psi$. The XY order parameter will still be decomposed into damped part and undamped part, although both parts will only have discrete rotation symmetry.

We have used the edge states of 3d TBI as the example of helical FL, our analysis is applicable to other helical FL. For instance, if we give graphene a small but finite chemical potential, we can consider the spontaneous generation of order $\bar{\psi} \vec{\gamma} \mathcal{T}^a \psi$. $\mathcal{T}^a \in \text{SU}(4)$ is the flavor symmetry matrix operating on the real spin and Dirac cone valley space. The gamma matrices γ_i which operate on the two sublattices plays the role as the helical spin in our analysis, and the results in our paper are still applicable. Our study can also be applied to the Rashba model in Eq. 1, as long as the momentum \vec{q} carried by the boson field $\vec{\phi}_{\vec{q}}$ is much smaller than the distance between the two fermi surfaces of Rashba model: $\vec{q} \ll |\vec{K}_{f,out}| - |\vec{K}_{f,in}|$, therefore $\vec{\phi}$ does not induce coupling between the two fermi surfaces. One important difference between the Rashba model and the edge states of TBI is that, the uniform and static susceptibility is nonzero for Rashba model, although the transverse and longitudinal modes still gain the same uniform and static correction.

Generalization of these results to other spin-orbit coupled electron models is straightforward. The most general form of spin-orbit coupled electron model is

$$H = \frac{k^2}{2m} + \sum_a \beta B(\vec{k})_a \cdot \sigma_a. \quad (18)$$

When $B(\vec{k})_a$ takes the p -wave form $B_a \sim \epsilon_{ab} k_b$, the model becomes the Rashba model. For example, let us consider the following model as a 3d version of Rashba model: $B_a \sim k_a$, $a = x, y, z$. This model also has inner and outer fermi surfaces with hedgehog spin distribution around the fermi surface. The system has $O(3)$ rotation symmetry as long as spin and space rotation are synchronized. It would be interesting to consider the spontaneous breaking of this continuous symmetry by developing nonzero order of $\vec{\phi} = (\phi_x, \phi_y, \phi_z)$. After integrating out the fermions, just like the two dimensional cases we considered above, the vector $\vec{\phi}$ is decomposed into one longitudinal mode and two transverse modes. At the

quantum critical point, the longitudinal mode is a $z = 2$ propagating mode while the two transverse modes are $z = 3$ over-damped modes. We can also consider the possibility of d -wave $B(\vec{k})_a$, for instance $B_x \sim k_x^2 - k_y^2$, $B_y \sim 2k_x k_y$, which can be realized in hole-doped GaAs quantum well with inversion symmetric confining potential [27]. The result of our paper is still applicable to this model as long as we define the projection matrix in Eq. 10 and Eq. 11 as $P_{ab} \sim B_a B_b / (B_a^2 + B_b^2)$.

As a summary, in this work we discussed the spontaneous breaking of the continuous spin-space combined rotation symmetry in helical fermi liquid. we calculated the quantum critical modes at the quantum critical point, and the Goldstone mode in the ordered phase, as well as their effects on the quasiparticles. However, as was mentioned already, higher order loop diagrams may lead to more singular momentum and frequency dependent terms which have the potential to destroy the Gaussian fixed point studied in our paper. Therefore the analysis of the Gaussian fixed point in this paper is the basis of our future studies.

[1] E. I. Rashba, Sov. Phys. Solid State **2**, 1106 (1960).
 [2] Y. A. Bychkov and E. I. Rashba, J. Phys. C **17**, 6039 (1984).
 [3] H. Zhang, C.-X. Liu, X.-L. Qi, X. Dai, Z. Fang, and S.-C. Zhang, Nature Phys. **5**, 438 (2009).
 [4] Y. L. Chen, J. G. Analytis, J. H. Chu, Z. K. Liu, S. K. Mo, X. L. Qi, H. J. Zhang, D. H. Lu, X. Dai, Z. Fang, et al., arXiv:0904.1829 (2009).
 [5] L. Fu, C. L. Kane, and E. J. Mele, Phys. Rev. Lett. **98**, 106803 (2007).
 [6] L. Fu and C. L. Kane, Phys. Rev. Lett. **100**, 096407

(2008).
 [7] D. Hsieh, Y. Xia, D. Qian, L. Wray, J. H. Di, F. Meier, L. Patthey, J. Osterwalder, A. Fedorov, H. Lin, et al., arXiv:0904.1260 (2009).
 [8] D. A. Pesin and L. Balents, arXiv:0907.2962 (2009).
 [9] R. Li, J. Wang, X. Qi, and S.-C. Zhang, arXiv:0908.1537 (2009).
 [10] J. A. Hertz, Phys. Rev. B **14**, 1165 (1976).
 [11] A. J. Millis, Phys. Rev. B **48**, 7183 (1993).
 [12] C. Xu, arXiv:0908.2147 (2009).
 [13] B. A. Bernevig, X. Yu, and S.-C. Zhang, Phys. Rev. Lett. **95**, 076602 (2005).
 [14] S. Raghu, S. B. Chung, X.-L. Qi, and S.-C. Zhang, arXiv:0909.2477 (2009).
 [15] M. Campostrini, M. Hasenbusch, A. Pelissetto, P. Rossi, and E. Vicari, Phys. Rev. B **63**, 214503 (2001).
 [16] M. Vojta, Y. Zhang, and S. Sachdev, Phys. Rev. Lett. **85**, 4940 (2000).
 [17] M. Vojta, Y. Zhang, and S. Sachdev, Int. J. Mod. Phys. B **14**, 3719 (2000).
 [18] Y. Huh and S. Sachdev, Phys. Rev. B **78**, 064512 (2008).
 [19] V. Oganesyan, S. A. Kivelson, and E. Fradkin, Phys. Rev. B **64**, 195109 (2001).
 [20] D. Belitz, T. R. Kirkpatrick, and T. Vojta, Phys. Rev. B **55**, 9452 (1997).
 [21] A. Abanov and A. Chubukov, arXiv:cond-mat/0409601 (2004).
 [22] C. M. Varma, P. B. Littlewood, S. Schmitt-Rink, E. Abrahams, and A. E. Ruckenstein, Phys. Rev. Lett. **63**, 1996 (1989).
 [23] S.-S. Lee, arXiv: 0905.4532 (2009).
 [24] J. Polchinski, Nucl. Phys. B **422**, 617 (1994).
 [25] H.-J. Zhang, C.-X. Liu, X.-L. Qi, X.-Y. Deng, X. Dai, S.-C. Zhang, and Z. Fang, arXiv:0901.2762 (2009).
 [26] L. Fu, arXiv:0908.1418 (2009).
 [27] X.-L. Qi, Y.-S. Wu, and S.-C. Zhang, Phys. Rev. B **74**, 085308 (2006).